Journal of Rehabilitation in Civil Engineering 7-3 (2019) 103-116

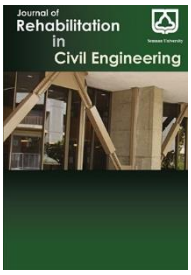

journal homepage: http://civiljournal.semnan.ac.ir/

A Target Displacement for Pushover Analysis to Estimate Seismic Demand of Eccentrically Braced Frames

A. Fakhraddini[1], M. J. Fadaee[2*] and H. Saffari[2]

1. Shahid Bahonar University of Kerman, Kerman, Iran

2. Department of Civil Engineering, Shahid Bahonar University of Kerman, Kerman, Iran

Corresponding author: *mjfadaee@uk.ac.ir*

ARTICLE INFO

Article history:
Received: 17 December 2017
Accepted: 14 July 2018

Keywords:
Pushover Analysis,
Seismic Assessment,
Target Displacement,
Eccentrically Braced Frames.

ABSTRACT

A main challenge for performance-based seismic engineering is to develop simple, practical and precise methods for assessing existing structures to satisfy considerable performance objectives. Pushover analysis is a simplified nonlinear analysis technique that can be implemented for estimating the dynamic demands imposed on a structure under earthquake excitations. In this method, structure is subjected to specified load pattern to reach a target displacement. The present study provides a target displacement for estimating the seismic demand of eccentrically braced frames (EBFs). A parametric study is conducted on a group of 30 EBFs under a set of 15 accelerograms. The results of nonlinear dynamic analyses of EBFs have been post-processed by nonlinear regression analysis and a relation is proposed for target displacement. In order to verify the capability of the proposed procedure, three EBFs are assessed by the present method in which the results show that the proposed method is capable of reproducing the peak dynamic responses with relatively good accuracy. Additionally, the comparison of obtained results with those of other conventional target displacement methods such as N2 method, and displacement coefficient method confirms the efficiency of the suggested one.

1. Introduction

Formerly, elastic analysis was the major tool in seismic design of structures. However, behavior of structures during severe earthquakes indicates that relying on just elastic analysis is not adequate. Alternatively, nonlinear dynamic analysis, while provides accurate results, is time consuming and such

DOI: 10.22075/JRCE.2018.13427.1245

analysis must be repeated for a group of acceleration time histories and needs extensive interpretation of results. Researchers have long been interested in developing prompt and practical methods to simulate nonlinear behavior of structures under earthquake loads. During the last decade, the nonlinear static pushover analysis has been gaining ground among the structural engineering society as an alternative mean of analysis. The purpose of the pushover analysis is to assess the structural performance by estimating the strength and deformation capacities using static nonlinear analysis and comparing these capacities with the demands at the corresponding performance levels. The assessment is based on the estimation of important structural parameters, such as global and inter-story drift, element deformations and internal forces. The analysis accounts for the geometrical nonlinearity and material inelasticity, as well as the redistribution of the internal forces.

In static pushover analysis, the starting point is to calculate a target displacement and a predefined lateral load pattern. Subsequently, a static analysis of the structural model is carried out to reach the target displacement. The load pattern is applied step by step until structure reaches a predetermined target displacement. Various target displacements are recommended in valid codes to perform a pushover analysis. One of the first steps taken in this approximate solution is to assess the maximum roof displacement, known as target displacement.

Typically, the traditional procedure is to push the structure with a target displacement such as capacity spectrum, and coefficient method by means of a lateral load distribution. The capacity spectrum method (CSM) [1] is known as a seismic evaluation method in some guidelines [2, 3]. This method is able to predict the demands of forces and deformations of low to medium buildings. Some researchers in earthquake engineering have made lots of efforts to develop the related theory and application for pushover analysis. Fajfar [4] proposed a comprehensive, relatively simple, N2 method for seismic damage analysis of reinforced concrete buildings. The N2 method as a special form of the CSM has been implemented in the Eurocode-8 [5], in which the demand is represented by an inelastic spectrum. Chopra and Goel [6, 7] established the demand diagram of an inelastic system according to the constant-ductility inelastic response spectra, and calculated the ductility factor of the system based on the intersection point of capacity and demand diagrams. Gencturk and Elnashai [8] developed an advanced CSM, incorporating the inelastic response history analysis of SDOF system, in which the updating bilinear idealization of structural system according to the selected trial performance point on the capacity diagram improves the accuracy of CSM. Displacement Coefficient Method (DCM) defined in ASCE41-13 [9] is based on the capacity diagram derived from static pushover analysis. However, these methods for estimating seismic demands have some drawbacks [10-11].

The principal objective of this study is to provide a pushover analysis procedure based on a new target displacement for estimating seismic demands of steel eccentrically braced frames. For this purpose, a parametric study is conducted on a group of 30 EBFs under a set of 15 far-field and near-field accelerograms scaled to different amplitudes to adapt various performance levels. The results of nonlinear dynamic analyses of

EBFs have been post-processed by nonlinear regression analysis in order to extract relation for target displacement. The capability and validity of proposed method is evaluated through nonlinear dynamic analysis as benchmark solutions. The results indicate that the proposed method has good estimation of inter-story drifts rather than those of N2, and DCM.

2. Review of Some Existing Methods of Target Displacement

2.1 Displacement Coefficient Method

Displacement Coefficient Method (DCM) expressed in ASCE41-13 [9] is based on the capacity diagram derived from static pushover analysis. In this technique, the greatest displacement demand is obtained using some coefficients. Target displacement is shown by δt. Computation of performance point is depicted in Fig. 1 [9]. The target roof displacement can be determined as follows:

$$\delta_t = C_0 C_1 C_2 S_a \left(\frac{T_e^{\,2}}{4\pi^2}\right) g \qquad (1)$$

where C_0 is a modification factor that relates spectral displacement of an equivalent single-degree-of-freedom (SDOF) system to the roof displacement of the multi-degree-of-freedom (MDOF) system, C_1 is a modification factor to relate expected maximum inelastic displacements to displacements calculated from a linear elastic analysis, C_2 is a modification factor to represent the effect of hysteretic behavior on the maximum displacement response, S_a is the response spectrum acceleration at the effective fundamental vibration period and damping ratio of the building under consideration, and T_e is the effective fundamental period of the structures.

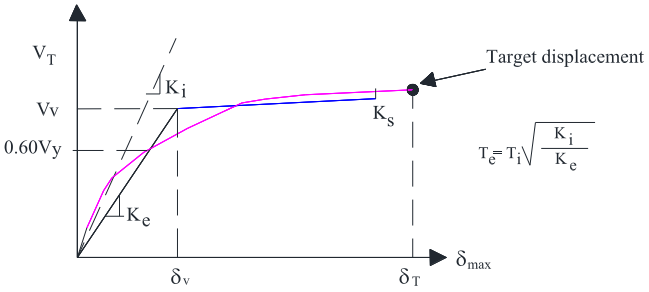

Fig. 1. Determination of performance point by DCM [9].

2.2. N2 Method

One of simplified nonlinear methods is the N2 method [4, 5]. The N2 method combines pushover analysis of a MDOF system with the response spectrum analysis of an equivalent SDOF model. According to the N2 method, the following procedure is employed in order to compute the peak floor displacements of the EBFs.

In this method, in order to obtain the capacity diagram, the frame is pushed with a target displacement equal to 10 percent of the structure's height at the first step. The 15 selected ground motions are scaled for three performance levels and response spectra resulting from each of records are drawn. Inelastic demand spectra are determined from the elastic design spectra [12] and converted into acceleration displacement response spectra (ADRS) format that provides the demand spectrum. The intersection of the capacity spectrum and demand spectrum provides an estimate of the inelastic acceleration and displacement demand. Capacity diagrams are idealized with elastic–perfectly plastic curves. (Fig. 2).

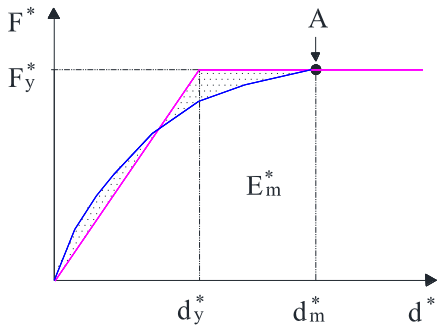

Fig. 2. Idealization of capacity curve by N2 method [5].

3. Parametric Study

3.1. Description of the Case Study Structures

In order to obtain relation for the target displacement, a group of thirty eccentrically braced frames has been used. Typical configuration of 2-D frames is shown in Fig. 3. The uniform story height and bay length are 360 and 900 cm, respectively. The number of stories of the frames, ns, takes the values 3, 6, 9, 12 and 15. Taking the link length, e, equal to aL (see Fig. 3), six values, 0.1, 0.2, 0.3, 0.4, 0.5 and 0.6 are assigned for parameter a, in the design phase.

All frames have three bays with simple beam-to-column connections. The uniform dead and live loads of all beams are 2.1 and 1.05 ton/m, respectively. The EBFs have been designed based on AISC 360-10 [13], AISC 341-10 [14] and ASCE7-10 [15] using ETABS [16] software. All frames are assumed to be founded on firm soil, class C of NEHRP, and located in the region of highest seismicity. The yield strength of steel is assumed as 3515 kg/cm2 for all structural members. Final section sizes of all frames are summarized in Table 1. In this table, phrases like 3(14x311) +3(14x132) show that the first three stories possess columns with W14x311 section sizes, while the three higher stories possess columns with W14x132 section sizes.

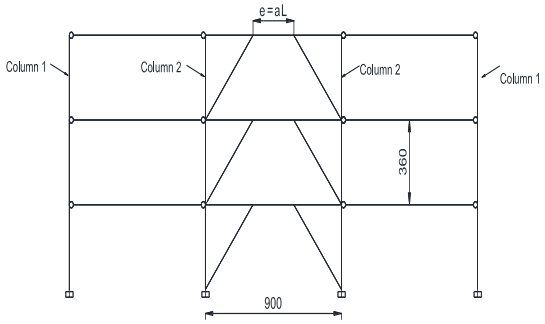

Fig. 3. Typical configuration of EBFs.

3.2. Earthquke Ground Motions

Fifteen different ground motions are considered for the nonlinear time history analysis of this study. This category includes both far-field and near-field records [17]. The near-field ground motion selected from SAC [18] database and far-field records selected from FEMA P695 [19]. The records are available in the Pacific Earthquake Engineering Research (PEER) site, http://peer.berkeley.edu/smcat. The basic parameters of the records are summarized in Table 2 as well as their elastic response spectra shown in Fig. 4.

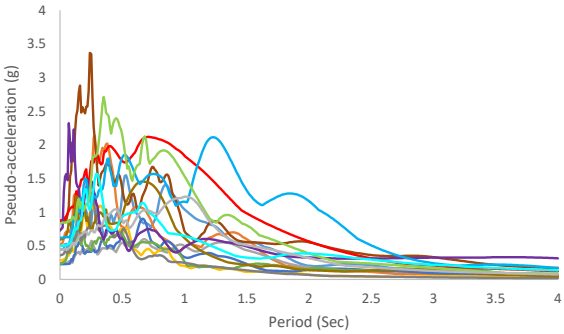

Fig. 4. Acceleration spectra of the 15 selected records.

Table 1. Section sizes of the EBFs.

n	Link length $a=e/L$	Column1*	Column2*	Link beam*	Gravity beam* (all stories)	brace**	Periods (Sec.) T_1, T_2, T_3
3-StoryEBFs	0.1	3(14x30)	3(14x132)	3(14x48)	14x109	2(6x1/2)+6x1/4	0.45,0.17,0.10
	0.2	3(14x30)	3(14x132)	14x53+2(14x48)	14x109	6x1/2+2(6x1/4)	0.64,0.23,0.14
	0.3	3(14x30)	3(14x132)	2(14x53)+14x48	14x109	6x1/2+2(6x1/4)	0.66,0.27,0.14
	0.4	3(14x30)	3(14x132)	2(14x68)+14x53	14x109	8x1/2+6x1/2+6x1/4	0.67,0.29,0.14
	0.5	3(14x30)	3(14x176)	2(14x68)+14x53	14x109	8x1/2+6x1/2+6x1/4	0.72,0.31,0.16
	0.6	3(14x30)	3(14x176)	2(14x132)+14x82	14x109	2(6x1/2)+6x1/4	1.01,0.33,0.18
6-StoryEBFs	0.1	3(14x38)+ 3(14x30)	3(14x311)+ 3(14x132)	2(14x53)+ 3(14x48)	14x109	5(6x1/2)+ 6x1/4	0.81,0.28,0.17
	0.2	3(14x38)+ 3(14x30)	3(14x311)+ 3(14x132)	2(14x68)+ 4(14x48)	14x109	3(6x1/2)+ 3(6x1/4)	1.01,0.40,0.23
	0.3	3(14x38)+ 3(14x30)	3(14x311) +3(14x132)	4(14x68)+ 2(14x48)	14x109	3(6x1/2)+ 3(6x1/4)	1.10,0.42,0.26
	0.4	3(14x38)+ 3(14x30)	3(14x311)+ 3(14x132)	14x82+2(14x74)+ 2(14x68)+14x48	14x109	4(6x1/2)+ 2(6x1/4)	1.13,0.45,0.26
	0.5	3(14x38)+ 3(14x30)	3(14x426)+ 3(14x176)	2(14x132)+ 4(14x68)	14x109	4(6x1/2)+ 2(6x1/4)	1.29,0.58,0.33
	0.6	3(14x38)+ 3(14x30)	3(14x426)+ 3(14x176)	4(14x132)+ 2(14x68)	14x109	4(6x1/2)+ 2(6x1/4)	1.60,0.61,0.33
9-StoryEBFs	0.1	3(14x48)+ 3(14x38)+ 3(14x30)	3(14x500)+ 3(14x311)+ 3(14x132)	4(14x53)+ 5(14x48)	14x109	7(6x1/2)+ 2(6x1/4)	1.23,0.44,0.25
	0.2	3(14x48)+ 3(14x38)+ 3(14x30)	3(14x500)+ 3(14x311)+ 3(14x132)	3(14x68)+ 2(14x53)+ 4(14x48)	14x109	7(6x1/2)+ 2(6x1/4)	1.42,0.58,0.33
	0.3	3(14x48)+ 3(14x38)+ 3(14x30)	3(14x500)+ 3(14x311)+ 3(14x132)	6(14x68)+ 14x53+ 2(14x48)	14x109	6(6x1/2)+ 3(6x1/4)	1.54,0.58,0.35
	0.4	3(14x48)+ 3(14x38)+ 3(14x30)	3(14x500)+ 3(14x311)+ 3(14x132)	3(14x82)+ 2(14x74)+ 3(14x68)+14x48	14x109	7(6x1/2)+ 2(6x1/4)	1.59,0.62,0.36
	0.5	3(14x48)+ 3(14x38)+ 3(14x30)	3(14x665)+ 3(14x426)+ 3(14x176)	5(14x132)+ 14x82+3(14x68)	14x109	6(6x1/2)+ 3(6x1/4)	1.61,0.72,0.40
	0.6	3(14x48)+ 3(14x38)+ 3(14x30)	3(14x665)+ 3(14x426)+ 3(14x176)	7(14x132) +2(14x68)	14x109	7(6x1/2)+ 2(6x1/4)	1.63,0.78,0.44
12-StoryEBFs	0.1	3(14x61)+ 3(14x48)+ 3(14x38)+ 3(14x30)	3(14x665)+ 3(14x500)+ 3(14x311)+ 3(14x132)	4(14x68)+ 2(14x53)+ 6(14x48)	14x109	9(6x1/2)+ 3(6x1/4)	1.62,0.56,0.33
	0.2	3(14x61)+ 3(14x48)+ 3(14x38)+ 3(14x30)	3(14x665)+ 3 (14x500)+ 3(14x311)+ 3(14x132)	8(14x68)+ 4(14x48)	14x109	9(6x1/2)+ 3(6x1/4)	1.71,0.74,0.41
	0.3	3(14x61)+ 3(14x48)+ 3(14x38)+ 3(14x30)	3(14x665)+ 3(14x500)+ 3(14x311)+ 3(14x132)	3(14x132)+ 4(14x82)+ 3(14x74)+ 2(14x68)	14x109	9(6x1/2)+ 3(6x1/4)	1.87,0.80,0.42
	0.4	3(14x61)+ 3(14x48)+ 3(14x38)+ 3(14x30)	3(14x665)+ 3(14x500)+ 3(14x311)+ 3(14x132)	3(14x132)+ 4(14x82)+ 3(14x74)+ 2(14x68)	14x109	8x1/2+ 8(6x1/2)+ 3(6x1/4)	1.99,0.88,0.44
	0.5	3(14x61)+ 3(14x48)+ 3(14x38)+ 3(14x30)	3(14x730)+ 3(14x665)+ 3(14x426)+ 3(14x176)	9(14x132)+ 14x82+ 14x74+ 14x68	14x109	6(8x1/2)+ 3(6x1/2)+ 3(6x1/4)	2.08,0.90,0.45
	0.6	3(14x61)+ 3(14x48)+ 3(14x38)+ 3(14x30)	3(14x730)+ 3(14x665)+ 3(14x426)+ 3(14x176)	6(14x132)+ 6(14x132)	14x109	7(8x1/2)+ 3(6x1/2)+ 2(6x1/4)	2.14,0.98,0.51
15-Story	0.1	3(14x68)+ 3(14x61)+ 3(14x48)+	3(14x730)+ 3(14x665)+ 3(14x500)+	8(14x68)+ 2(14x53)+ 5(14x48)	14x109	5(8x1/2)+ 8(6x1/2)+ 2(6x1/4)	1.93,0.67,0.38

	3(14x38)+ 3(14x30)	3(14x311)+ 3(14x132)				
0.2	3(14x68)+ 3(14x61)+ 3(14x48)+ 3(14x38)+ 3(14x30)	3(14x730)+ 3(14x665)+ 3(14x500)+ 3(14x311)+ 3(14x132)	14x132+ 2(14x82)+ 3(14x74)+ 9(14x68)	14x109	5(8x1/2)+ 8(6x1/2)+ 2(6x1/4)	2.02,0.75,41
0.3	3(14x68)+ 3(14x61)+ 3(14x48)+ 3(14x38)+ 3(14x30)	3(14x730)+ 3(14x665)+ 3(14x500)+ 3(14x311)+ 3(14x132)	7(14x132)+ 3(14x82)+ 2(14x74)+ 2(14x68)	14x109	5(8x1/2)+ 8(6x1/2)+ 2(6x1/4)	2.13,0.75,0.41
0.4	3(14x68)+ 3(14x61)+ 3(14x48)+ 3(14x38)+ 3(14x30)	6(14x730)+ 3(14x500)+ 3(14x370)+ 3(14x145)	10(14x132)+ 14x82+ 14x74+ 3(14x68)	14x109	7(8x1/2)+ 6(6x1/2)+ 2(6x1/4)	2.30,0.81,0.43
0.5	3(14x68)+ 3(14x61)+ 3(14x48)+ 3(14x38)+ 3(14x30)	6(14x730)+ 3(14x665)+ 3(14x426)+ 3(14x176)	2(14x159)+ 3(14x145)+ 7(14x132)+ 14x82+ 14x74+14x68	14x109	9(8x1/2)+ 5(6x1/2)+ 6x1/4	2.42,0.85,0.46
0.6	3(14x68)+ 3(14x61)+ 3(14x48)+ 3(14x38)+ 3(14x30)	6(14x730)+ 3(14x665)+ 3(14x426)+ 3(14x176)	5(14x176)+ 2(14x159)+ 2(14x145)+ 5(14x132)+ 14x68	14x109	11(8x1/2)+ 3(6x1/2)+ 6x1/4	2.56,0.88,0.51

* These elements, are W-type pattern. ** These elements, are HSS-type pattern.

Table 2. Characteristics of earthquake ground motions.

Event	Magnitude	Mechanism	Rjb (km)	PGA (g)
RSN821_ERZINCAN_ERZ-EW	6.69	Strike slip	0	0.49
RSN1106_KOBE_KJM000	6.9	Strike slip	0.94	0.83
RSN1120_KOBE_TAK000	6.9	Strike slip	1.46	0.62
RSN879_LANDERS_LCN260	7.28	Strike Slip	2.19	0.72
RSN3548_LOMAP_LEX000	6.93	Reverse Oblique	3.22	0.44
RSN828_CAPEMEND_PET000	7.01	Reverse	0	0.59
RSN1063_NORTHR_RRS228	6.69	Reverse	0	0.87
RSN143_TABAS_TAB-L1	7.35	Reverse	1.79	0.85
RSN125_FRIULI.A_A-TMZ000	6.5	Reverse	14.97	0.35
RSN169_IMPVALL.H_H-DLT262	6.53	Strike Slip	22.03	0.23
RSN1116_KOBE_SHI000	6.9	Strike Slip	19.14	0.22
RSN848_LANDERS_CLW-LN	7.28	Strike Slip	19.74	0.28
RSN900_LANDERS_YER270	7.28	Strike Slip	23.62	0.24
RSN752_LOMAP_CAP000	6.93	Reverse Oblique	15.23	0.51
RSN953_NORTHR_MUL009	6.69	Reverse	9.44	0.44

3.3. Computational Methodology and Framewrk of the Present Study

The 30 EBFs of Table 1 are analyzed to determine their response to each of the 15 seismic excitations of Table 2. The OPENSEES [20] software has been employed for the nonlinear time history analyses. In EBFs, the inelastic response of link beam has been modeled by means of the approach that proposed by Bosco et. al [21]. The model simulates the effect of the shear force and flexural bending on the inelastic behavior of the link beams with short, intermediate and long length.

The link model includes five elements connected in series as shown in Fig. 5. The middle element (EL0) has the identical length and moment of inertia of the link and takes the flexural elastic response of the link into account. There are two zero length elements (EL1 and EL2) in this simulation. Whereas (EL1) considers the elastic and inelastic shear response of half a link, (EL2) considers the inelastic flexural response of

the ending part of the link. The nodes of EL1 and EL2 are permitted to have independently relative vertical displacements and relative rotations, respectively [21].

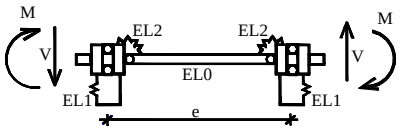

Fig. 5. Modelling of the link [21].

Beams, columns, braces and beam segments outside of the links are modelled with the aid of elastic elements to remain essentially elastic. Based on Bosco model [21], the materials of shear and flexural springs are defined as uniaxial material BrbDallAsta [20]. Elastic beam-column element is used to model beams and columns. Braces have been modeled by means of truss element. The Rayleigh damping is considered in the analyses. Stiffness and mass coefficients are specified in order that the first and the third modes of the frame are determined by an equivalent viscous damping factor equal to 0.05.

For each pair of frame and ground motion, the scale factors (SF) of the ground motion which correlate to a specific performance level are determined by Incremental Dynamic Analysis (IDA). The peak inter-story drifts have been recorded at the following performance levels based on acceptance criteria of ASCE 41-13 [9]:

- Immediate Occupancy (IO) of the frame (target drift = 0.005 or acceptance criteria of link rotation angle).
- Life Safety (LS) of the frame (target drift = 0.02 or acceptance criteria of link rotation angle).
- Collapse Prevention (CP) of the frame (target drift = 0.03 or acceptance criteria of link rotation angle)

The peak inter-story drifts at the time that the frame reaches to a desired performance level are recorded to generate the databank for EBFs. This procedure includes finding a scale factor (SFi, i=1, 2, 3) of the ground motion for each pair of EBF and ground motion, such that the response of the frame to be in the performance level [22-28]. Subsequently, the ground motion is multiplied by SFi and through running three nonlinear time history analyses. Finally, the corresponding three peak inter-story drift patterns of each frame are derived.

3.4. Proposed Target Displacement in Pushover Analysis

In the following section, simple formula is proposed to estimate an approximate target displacement in regular EBFs. The target displacement of each pair of frame and ground motion is obtained by the summation of the peak inter-story drift at each floor.

$$\delta_t = \sum_{i=1}^{n} \Delta_i \quad (2)$$

where δ_t is the target displacement of the roof and Δ_i is the peak inter-story drift at *i*th floor. The Levenberg-Marquardt algorithm of SPSS software [29] is employed for nonlinear regression analysis. By analyzing the response databank, it is specified that, the main parameters affecting the target displacement are the number of stories (n), performance level and the ratio of link length (e) to span length (L). Therefore, a proposed formula is developed for estimating of the target displacement of EBFs based on displacement coefficient method [9].

$$\delta_t = C_0 C_1 IDR.\left(\frac{e}{L}\right)^{0.2} 20n^{0.45}\left(S_a \frac{T^2}{4\pi^2}\right)g \quad (3)$$

where *IDR* (Inter-story Drift Ratio) relates the performance level to the target displacement, *g* is acceleration of gravity, S_a is pseudo acceleration spectrum and *T* is the fundamental period.

It is worth noting that nonlinear regression for matching nonlinear random functions is based on the data derived from independent variables to reach the maximum value of the coefficient of determination (R^2). R^2 is the proportion of the variance in the dependent variable that is predictable from the independent variables. In this study, the coefficient R2 for Eq. (3) is taken equal to 92.2.

4. Validation of the Proposed Method

In order to assess the accuracy of the proposed target displacement, the results obtained with the approximate method is compared with the responses computed with nonlinear time history analyses as benchmark solution. Nonlinear dynamic analyses have been performed by means of OPENSEES software [20] as benchmark results.

4.1. Description of Tested Frames

The EBFs selected in this study consist of regular 4, 8, and 16-story EBFs which were previously studied by Speicher and Harris [30]. For all frames, the height of the first floor is 18 feet and other floor heights are 14 feet and gravity loads are considered based on Speicher and Harris study [30]. In all frames, the brace-to-beam and the beam-to-column connections are fully restrained [31-33].

All frames are assumed to be based on firm soil, class C of NEHRP. Corresponding seismic design parameters utilized for the EBFs are provided in Table 3. A steel grade of A992 that has a yield strength of 3515 kg/cm2 is used in the design of all structural members. Other properties of frames are listed in Table 4 and section sizes of all frames are shown in Fig. 6. These frames are evaluated in life safety performance level [9].

4.2. Set of Tested Earthquake Ground Motion Records

In order to establish a benchmark response to examine the validity of the proposed pushover analyses, nonlinear time-history analyses are conducted on the same set of frames. For this purpose, a set of ground motions is used for nonlinear time history assessment as test records. Ten SAC Los Angeles ground motions [34] corresponding to 10% probabilities of exceedance in a 50-year period are considered for the nonlinear dynamic analysis. Details of these records are presented in Table 5 and their five-percent damped elastic acceleration spectra are shown in Fig.7

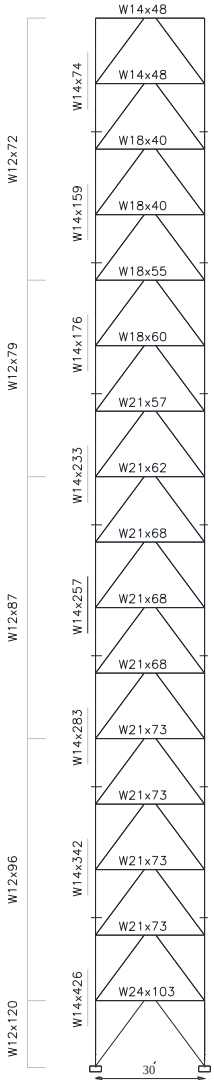

(a) 16-story

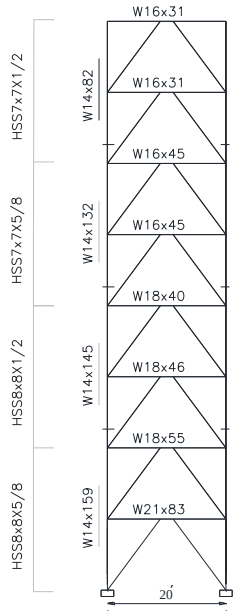

(b) 8-story

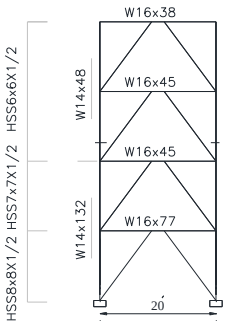

(c) 4-story

Fig. 6. Final properties obtained for EBFs.

Table 3. Seismic design parameters of EBFs.

Parameters	Values
Spectral response acceleration at short period, S_S	1.7865 g
Spectral response acceleration at period of 1.0 s, S_1	0.8589 g
Acceleration site coefficient, F_a	1.0
Velocity site coefficient, F_v	1.3
Design spectral response acceleration in the short period range, S_{DS}	1.191 g
Design spectral response acceleration at a period of 1.0 s, S_{D1}	0.744 g
Site class	C
Seismic design category	E

Table 4. Some properties of frames.

story	Bay width (cm)	Link length (cm)	Floor seismic weight (ton)
4	600	75	295
8	600	75	295
16	900	97.5	304

Table 5. Characteristics of selected earthquake ground motions.

SAC Name	Duration (sec.)	Magnitude (Mw)	Distance (km)	PGA (cm/sec^2)
LA01	39.38	6.9	10.0	445.0
LA02	39.08	6.9	10.0	652.5
LA04	39.08	6.5	4.1	471.0
LA06	39.08	6.5	1.2	226.5
LA09	79.98	7.3	25.0	501.7
LA12	39.98	7.0	12.4	936.0
LA13	59.98	6.7	6.7	654.5
LA16	14.95	6.7	7.5	560.0
LA17	59.98	6.7	6.4	550.0
LA19	59.98	6.0	6.7	984.0

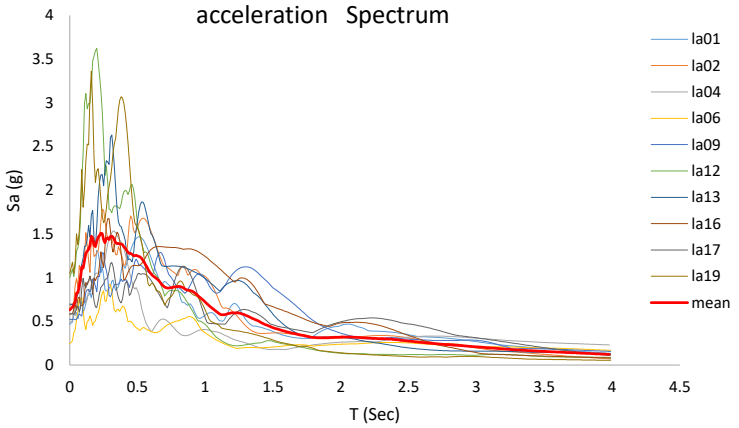

Fig. 7. Elastic acceleration response spectrum.

5. Description and Discussion of Results

In this section, 3 EBFs as example are evaluated in life safety performance level [9] and target drift ratio criteria of 2%. In Table 6, the values of target displacement of different methods have been listed. It can be seen that values of target displacement of proposed method in high-rise frames are more than N2, and less than displacement coefficient methods.

In Figs. 8 through 10 the peak inter-story drift profiles resulting from mean nonlinear dynamic analyses are compared with those obtained from different pushover analyses. For a better display and prevention of merging of curves only the mean responses of inter-story drift are drawn. It is observed that the inter-story drift responses of proposed method in high-rise frames at upper stories are greater than nonlinear dynamic analyses limits; the responses are in relatively good agreement with the mean values of peak inter-story drifts of nonlinear dynamic analyses in all studied frames. It is resulted, in general, the drift responses of proposed approach is better than N2 method and displacement coefficient method with code-compliant (ASCE/SEI 7-10) lateral load pattern [15].

Table 6. The values of target displacement in various methods (cm).

method frame	DCM	N2	Proposed	Nonlinear dynamic
16 Story	37.52	25.02	33.45	28.40
8 Story	27.60	15.20	18.55	17.70
4 Story	14.2	10.6	11.28	10.05

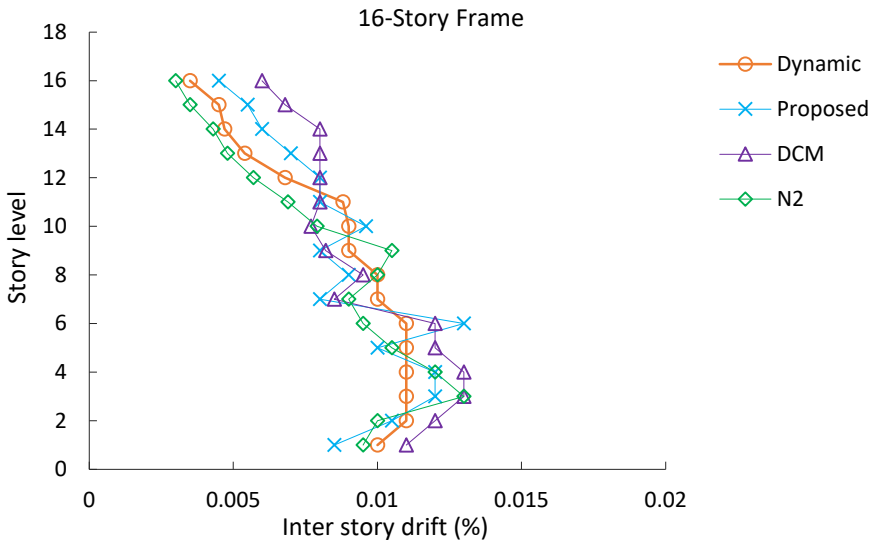

Fig. 8. Distribution of drift ratio resulting from the proposed method and the nonlinear dynamic analysis for 16-story frame.

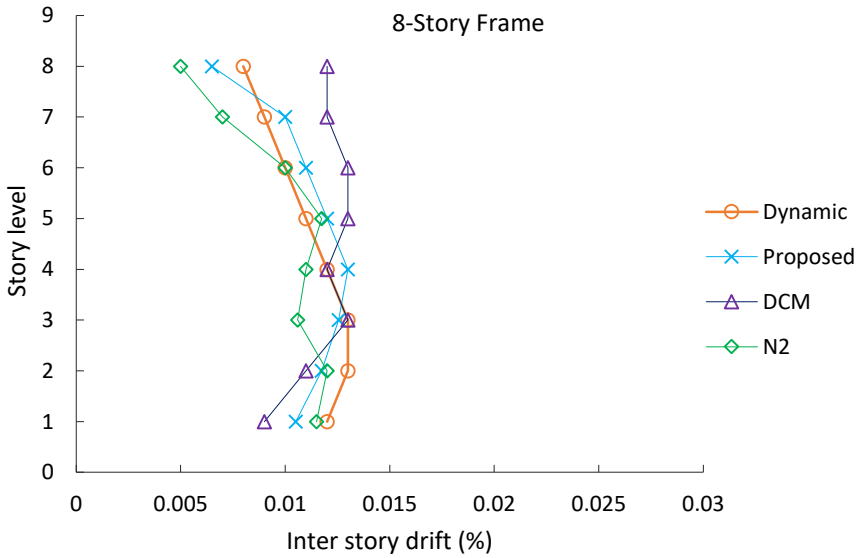

Fig. 9. Distribution of drift ratio resulting from the proposed method and the nonlinear dynamic analysis for 8-story frame.

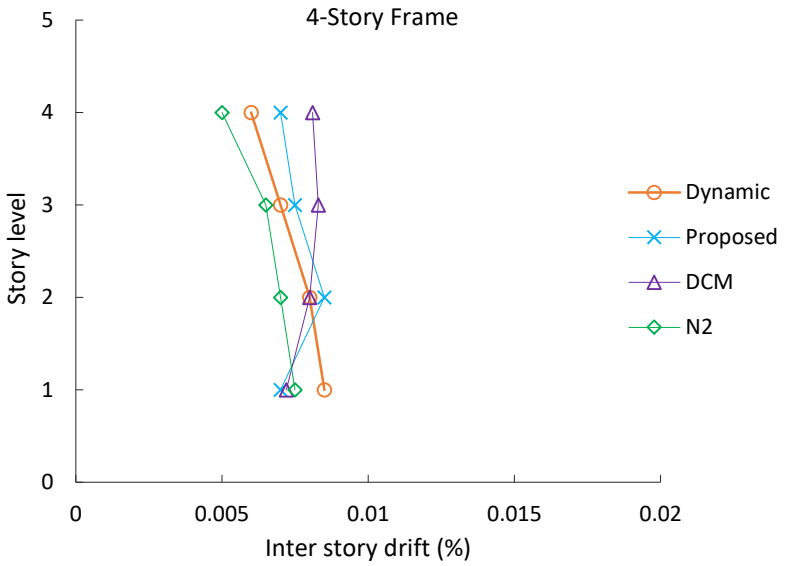

Fig. 10. Distribution of drift ratio resulting from the proposed method and the nonlinear dynamic analysis for 4-story frame.

6. Conclusion

This study presents a target displacement for pushover procedure in framework of performance based design. A parametric study is conducted on a group of 30 EBFs under a set of 15 far-field and near-field accelerograms. The results of nonlinear dynamic analyses of EBFs have been post-processed by nonlinear regression analysis and a relation for target displacement has been suggested.

The validity and capability of suggested configuration are assessed by comparison of the pushover response of practical examples with benchmark solutions based on nonlinear time history analyses. The nonlinear time history analyses results revealed that the proposed procedure estimates inter-story drift responses for the desired performance level with relatively good accuracy. It is shown that the proposed method leads to better responses rather than N2 method and displacement coefficient methods, particularly in high-rise buildings.

REFERENCES

[1] Freeman, SA., Nicoletti, JP., Tyrell JV. (1975). Evaluation of existing buildings for seismic risk class study of Puget Sound Naval Shipyard. In: Proceedings of first US national conference on earthquake engineering. Washington: Bremerton; p. 113-22.

[2] Applied Technology Council. (1996). Seismic evaluation and retrofit of concrete buildings. Report ATC-40. Redwood City (CA).

[3] Federal Emergence Management Agency. (2005). Improvement of nonlinear static seismic analysis procedure. Report FEMA-440. Washington (DC).

[4] Fajfar P. (1999). Capacity spectrum method based on inelastic demand spectra, Earthq Eng Struct Dyn; 28(9):979-93.

[5] Eurocode 8 (EC8). (2004). Design of Structures for Earthquake Resistance, Part 1: General Rules, Seismic Actions and

Rules for Buildings, European Standard EN 1998-1, Stage 51 Draft, European Committee for Standardization (CEN), Brussels.

[6] Chopra, AK., Goel, RK. (1999). Capacity-demand-diagram methods for estimating seismic deformation of inelastic structures: SDF systems. Report no. PEER-1999/02. Berkeley (CA): Pacific Earthquake Engineering Research Center. University of California.

[7] Chopra, AK., Goel, RK. (1999). Capacity-demand-diagram methods based on inelastic design spectrum, Earthq Spectra; 15(4):637-56.

[8] Gencturk, B., Elnashai, AS. (2008). Development and application of an advanced capacity spectrum method, Eng Struct; 30(11):3345-54.

[9] American Society of Civil Engineers, ASCE/SEI 41 (2013); Seismic evaluation and retrofit of existing buildings, Reston, VA.

[10] Krawinkler, H., Seneviratna, GDPK. (1998). Pros and cons of a pushover analysis of seismic performance evaluation, Eng Struct; 20(4-6):452-64.

[11] Kunnath, SK., Kalkan, E. (2004). Evaluation of seismic deformation demands using nonlinear procedures in multistory steel and concrete moment frames, ISET J. Earthquake Technol., 41(1), 159–182.

[12] Newmark, NM., Hall, WJ. (1982). Earthquake Spectra and Design, EERI Monograph Series, Earthquake Engineering Research Institute, Oakland, CA.

[13] AISC (American Institute of Steel Construction). (2010). Specification for Structural Steel Buildings, AISC 360-10, Chicago, IL.

[14] AISC (American Institute of Steel Construction), (2010). Seismic Provisions for Structural Steel Buildings, AISC 341-10, Chicago, IL.

[15] American Society of Civil Engineers, ASCE/SEI 7 (2010); Minimum design loads for buildings and other structures, Reston, VA.

[16] CSI. Extended three dimensional analysis of building systems. ETABS. Version 9.7.4 ed. (2015). Berkeley, CA: Computers and Structures, Inc.

[17] Karavasilis, TL., Bazeos, N., Beskos, DE. (2006). Maximum Displacement Profiles for the Performance-Based Seismic Design of Plane Steel Moment Resisting Frames. Engineering Structures, 28(1): 9–22.

[18] SAC Joint Venture. Develop suites of time histories, (1997). Project Task: 5.4.1, Draft Report, March 21, Sacramento, CA, USA.

[19] FEMA. (2009). Quantification of building seismic performance factors. FEMA P695. Washington, D.C.: Department of Homeland Security.

[20] PEER. Open system for earthquake engineering simulation: opensees. (2016). Berkeley: Pacific Earthquake Engineering Research Center (PEER). University of California; ⟨http://opensees.berkeley.edu⟩.

[21] Bosco, M., Marino, EM., Rossi, PP. (2015). Modelling of steel link beams of short, intermediate or long length, Engineering Structures; 84: 406–418.

[22] Saffari, H., Damroodi, M., Fakhraddini, A. (2017). Assessment of seismic performance of eccentrically braced frame with vertical members, Asian journal of civil engineering; 18(2): 255-269.

[23] Fakhraddini, A., Saffari, H., Fadaee, MJ. (2017). Peak displacement patterns for the performance-based seismic design of steel eccentrically braced frames, Earthquake Engineering & Engineering Vibration (accepted).

[24] Bazzaz M., Andalib Z., Kheyroddin A. and Kafi M.A. (2015a). Numerical Comparison of the Seismic Performance of Steel Rings in Off-centre Bracing System and Diagonal Bracing System, Journal of Steel and Composite Structures, Vol. 19, No. 4, 917-937.

[25] Bazzaz M., Andalib Z., Kafi M.A. and Kheyroddin A. (2015b). Evaluating the Performance of OBS-C-O in Steel Frames under Monotonic Load, Journal of

Earthquakes and Structures, Vol. 8 No.3, 697-710.

[26] Andalib Z., Kafi M.A., Kheyroddin A. and Bazzaz M. (2014). Experimental Investigation of the Ductility and Performance of Steel Rings Constructed from Plates, Journal of Constructional steel research, Vol. 103, 77-88.

[27] Bazzaz M., Kheyroddin A., Kafi M.A., Andalib Z. and Esmaeili H. (2014). Seismic Performance of Off-centre Braced Frame with Circular Element in Optimum Place, International Journal of Steel Structures, Vol 14, No 2, 293-304.

[28] Bazzaz M., Kheyroddin A., Kafi M.A. and Andalib Z. (2012). Evaluation of the Seismic Performance of Off-Centre Bracing System with Ductile Element in Steel Frames, Journal of Steel and Composite Structures, Vol 12, No 5, 445-464.

[29] IBM Corp. Released, IBM SPSS Statistics for Windows, (2013), Version 22.0. Armonk, NY: IBM Corp.

[30] Speicher, SM., Harris, III JL. (2016). Collapse prevention seismic performance assessment of new eccentrically braced frames using ASCE 41, Eng. Struct, 117, 344–357.

[31] Bazzaz M., Kafi M., Andalib Z. and Esmaeili H. (2011). Seismic Behavior of Off-centre Bracing Frame, 6th National Congress on Civil Engineering, Semnan, Iran, 26-27 Apr, in Persian.

[32] Andalib Z., Kafi M., Kheyroddin A. and Bazzaz M. (2011). Investigation on the Ductility and Absorption of Energy of Steel Ring in Concentric Braces, 2nd Conference on Steel & Structures, Tehran, Iran, December, in Persian.

[33] Andalib Z., Kafi M. A., and Bazzaz M. (2010). Using Hyper Elastic Material for Increasing Ductility of Bracing, 1st Conference of Steel & Structures and 2nd Conference on Application of High-Strength Steels in Structural Industry, Tehran, Iran, December, in Persian.

[34] Somerville, P., Smith, N., Punyamurthula, S., Sun, J. (1997). Development of ground motion time histories for phase 2 of the FEMA/SAC steel project. Report No. SAC/BD-97/04. Sacramento (California): SAC Joint Venture.